Chinese Physics C Vol. 41, No. 1 (2017) 014102

Systematic study of α preformation probability of nuclear isomeric and ground states*

Xiao-Dong Sun(孙小东)[1] Xi-Jun Wu(吴喜军)[1;1)] Bo Zheng(郑波)[2] Dong Xiang(向东)[2]
Ping Guo(郭萍)[1] Xiao-Hua Li(李小华)[2,3;2)]

[1] School of Math and Physics, University of South China, Hengyang 421001, China
[2] School of Nuclear Science and Technology, University of South China, Hengyang 421001, China
[3] Cooperative Innovation Center for Nuclear Fuel Cycle Technology & Equipment,
University of South China, Hengyang 421001, China

Abstract: In this paper, based on the two-potential approach combining with the isospin dependent nuclear potential, we systematically compare the α preformation probabilities of odd-A nuclei between nuclear isomeric states and ground states. The results indicate that during the process of α particle preforming, the low lying nuclear isomeric states are similar to ground states. Meanwhile, in the framework of single nucleon energy level structure, we find that for nuclei with nucleon number below the magic numbers, the α preformation probabilities of high-spin states seem to be larger than low ones. For nuclei with nucleon number above the magic numbers, the α preformation probabilities of isomeric states are larger than those of ground states.

Keywords: α decay, α preformation probability, nuclear isomer, two-potential approach

PACS: 21.60.Gx, 23.60.+e, 21.10.Tg **DOI:** 10.1088/1674-1137/41/1/014102

1 Introduction

Since the first observation of the nuclear isomers $^{234}\mathrm{Pa}^{\mathrm{m}}$ in 1921, a lot of nuclear structure information of isomeric states has being obtained [1–6]. Nuclear isomeric states are defined by their longer half-lives than other nuclear excitations [1]. Moreover, the nuclear isomers can be treated as steeping stones towards the island of stability, based on the understanding of the underlying single nucleon structure of super-heavy elements [6]. Some nuclear isomers in excited states are even more stable than the ground states, such as $^{180}\mathrm{Ta}^{\mathrm{m}}$ [1]. Whether nuclei have isomeric states depends on both collective motion of the nucleons as a whole and on single nucleon motion. Vibration and rotation of strongly deformed nuclei usually dominates the low energy and large angular momentum structure. These kinds of nuclear isomers are called shape or K isomers, and are distributed around $^{178}\mathrm{Hf}^{\mathrm{m}}$ far away from the spherical shell closures [1]. Another common kind of isomer related to single nucleon motion is spin trap isomers [1]. The existence of high-spin states can be explained by the nuclear shell model [1]. With increasing of level density below shell closures, the configuration where an unpaired nucleon occupies a quasi-degenerate high-spin orbit becomes common. An example is ^{167}Ir below the $Z=82$ shell closure, where the ground state is assigned as a $(\pi s_{1/2})^{+1}$ configuration and the isomeric state is assigned as a $(\pi h_{11/2})^{-1}$ configuration [7]. $^{167}\mathrm{Ir}^{\mathrm{m}}$ tends to convert through α decay to the corresponding daughter nucleus in high-spin states but not de-excitation through γ decay to ^{167}Ir in low-spin states [7]. Similarly, ^{167}Ir might well decay to the low-spin daughter state ^{163}Re. Therefore, it is interesting to study whether the spin-parity state of the parent nucleus influences the α preformation probabilities or not.

α decay has long been treated as an open source of nuclear structure information, such as the nuclear shell structure, properties of ground state, energy levels and low lying states, nuclear shape coexistence and so on [8–12]. Meanwhile, the α preformation probabilities contain a lot of nuclear structure information [13–16], and α decay is always one of the most powerful research tools to explore the neutron deficient nuclei and super-heavy

---

Received 2 July 2016, Revised 9 August 2016

* Supported by National Natural Science Foundation of China (11205083), Construct Program of Key Discipline in Hunan Province, Research Foundation of Education Bureau of Hunan Province, China (15A159), Natural Science Foundation of Hunan Province, China (2015JJ3103, 2015JJ2123), Innovation Group of Nuclear and Particle Physics in USC, Hunan Provincial Innovation Foundation for Postgraduate (CX2015B398)

1) E-mail: wuxijun1980@yahoo.cn

2) E-mail: lixiaohuaphysics@126.com (corresponding author)

element [17]. It is well known that the α transitions between ground states of even-even nuclei are onefold, e.g. $0^+ \rightarrow 0^+$. The unpaired nucleon in odd-A nuclei results in more complex α transitions, however, including favored and unfavored α decay. There are abundant nuclear isomers around the spherical shell closures at $Z = 82$ and $N = 126$, so we compare the α preformation probabilities between isomeric and ground states, taking into account the spin-parity state of the parent nuclei. The results show that most of the nuclei with high-spin states in a single shell have larger α preformation probabilities than low ones.

This article is organized as follows. In Section 2, the theoretical framework for the calculation of the α decay half-lives and the preformation probabilities is briefly described. The results and discussions are given in Section 3. In this section, at first, we systematically compare the α preformation probabilities of odd-A nuclei between the isomeric and ground states, and then from the framework of single nucleon level structure, the preformation probabilities of nuclei around shell closures are discussed in detail. A brief summary is given in Section 4.

2 Theoretical framework

The two-potential approach [18] for metastable states has been widely used to calculate α decay half-lives $T_{1/2}$, which are determined by the decay constant λ. It can be written as

$$T_{1/2} = \frac{\ln 2}{\lambda}. \tag{1}$$

The decay constant λ, which depends on the α particle preformation probability P_α, the penetration probability P, and the normalized factor F, can be expressed as

$$\lambda = \frac{\hbar P_\alpha F P}{4\mu}. \tag{2}$$

In the framework of the two-potential approach, the α particle assault frequency is obtained by normalizing the outgoing wave functions, while the generalized liquid drop model takes it by a classical approximation [19] and the effective liquid drop model puts it as a adjustable parameter [20]. The normalized factor F, determining the assault frequency, can be expressed as

$$F\int_{r_1}^{r_2} \frac{\mathrm{d}r}{2k(r)} = 1, \tag{3}$$

where r is the center-of-mass distance between the preformed α particle and the daughter nucleus. The r_1, r_2 and following r_3 are the classical turning points which satisfy the conditions $V(r_1) = V(r_2) = V(r_3) = Q_\alpha$. $k(r) = \sqrt{\frac{2\mu}{\hbar^2}\,|\,Q_\alpha - V(r)\,|}$ is the wave number. μ is the reduced mass of the α particle and daughter nucleus. $V(r)$ and Q_α are the total α-core potential and α decay energy, respectively. The penetration probability P, which is calculated by the WKB approximation [21], can be expressed as

$$P = \exp\left[-2\int_{r_2}^{r_3} k(r)\mathrm{d}r\right]. \tag{4}$$

The potential between the preformed α particle and the daughter nucleus $V(r)$, including nuclear, Coulomb and centrifugal potential, can be written as

$$V(r) = V_\mathrm{N}(r) + V_\mathrm{C}(r) + V_\mathrm{l}(r), \tag{5}$$

where $V_\mathrm{N}(r)$, $V_\mathrm{C}(r)$ and $V_\mathrm{l}(r)$ represent nuclear, Coulomb and centrifugal potential, respectively. In this work, we choose a type of cosh parameterized form for the nuclear potential [22]. It can be expressed as

$$V_\mathrm{N}(r) = -V_0\frac{1+\cosh(R/a)}{\cosh(r/a)+\cosh(R/a)}, \tag{6}$$

where V_0 and a are the depth and diffuseness of the nuclear potential, respectively. $V_\mathrm{C}(r)$ is the Coulomb potential and is taken as the potential of a uniformly charged sphere with sharp radius R, which can be expressed as

$$V_\mathrm{C}(r) = \begin{cases} \dfrac{Z_\mathrm{d}Z_\alpha e^2}{2R}\left[3-\left(\dfrac{r}{R}\right)^2\right] & r < R \\ \dfrac{Z_\mathrm{d}Z_\alpha e^2}{r} & r > R, \end{cases} \tag{7}$$

where Z_d and Z_α are proton number of the daughter nucleus and the α particle, respectively. The sharp radius R is given by

$$R = 1.28A^{1/3} - 0.76 + 0.8A^{-1/3}. \tag{8}$$

This empirical formula is commonly used to calculate α decay half-lives [23], which is derived from the nuclear droplet model and the proximity energy. The last part, centrifugal potential, can be estimated by

$$V_\mathrm{l}(r) = \frac{l(l+1)\hbar^2}{2\mu r^2}, \tag{9}$$

where l is the orbital angular momentum taken away by an α particle.

In our previous work, we have obtained a set of isospin dependent nuclear potential parameters, through analysing the experimental α decay half-lives of 164 even-even nuclei [24], which is a = 0.5958 fm and

$V_0 = 192.42 + 31.059\frac{N_\mathrm{d} - Z_\mathrm{d}}{A_\mathrm{d}}$ (MeV), where N_d, Z_d, and A_d denote the neutron, proton, and mass number of the daughter nucleus, respectively. The α preformation probability P_α abruptly decreases due to the nuclear shell effect and varies smoothly in the open-shell region [14]. Many studies also indicate that a smaller α particle preformation probability is required for odd-A nuclei than even-even nuclei due to the block effect [25]. Actually, P_α can be extracted from ratios of calculated α decay half-lives $T_{1/2}^{\mathrm{calc}}$ to experimental data $T_{1/2}^{\mathrm{expt}}$, which is defined as $P_\alpha = P_0 T_{1/2}^{\mathrm{calc}}/T_{1/2}^{\mathrm{expt}}$. The calculated half-lives are obtained under the assumption that α preformation probabilities keep constant for a given type of nucleus, such as even-even nuclei, odd-A nuclei, odd-odd nuclei. According to the calculations by using the density-dependent cluster model [25], the constant factor of preformation probability P_0 is taken as $P_0 = 0.43$ for even-even nuclei, $P_0 = 0.35$ for odd-A nuclei, and $P_0 = 0.18$ for doubly-odd nuclei.

3 Results and discussions

We calculate the α decay half-lives and the α preformation probabilities of odd-A nuclei for both isomeric and ground states. We also compare the α preformation probabilities between isomeric and ground states, both of which have the same number of protons and neutrons. Thus the influence of shell effect on the α preformation probability is identical. The only difference between isomeric and ground state is the spin-parity state of the parent nuclei. Most α transitions are favored decays. Then the preformed α particles consist of nucleons pairs, not unpaired nucleons. The detailed numerical results are given in the Tables 1–3, where Table 1 gives the results of odd(Z)-even(N) nuclei below the $Z = 82$ shell closure, covering ^{177,175}Au, ^{177}Tl, ^{167}Ir, and ^{153}Ho α decay lines of both isomeric and ground states. Table 2 gives the results of even(Z)-odd(N) nuclei below the $N = 126$ shell closure, including Hg, Pb, Po, Rn, and Ra isotopes. Table 3 gives the results of Bi, At, Fr isotopes of both ground and isomeric states in pairs. In all the tables, the first and second columns denote the α transition and the spin-parity transition, respectively. Nuclides with the upper suffix "m" indicate the isomeric states (with half-lives greater than 100 ns). The "()" in spin or parity means those quantities are uncertain, and the values with "#" are estimated from the trends in neighboring nuclides with the same Z or N parities. The next two columns stand for the decay energy Q_α (including the corresponding uncertainty) in units of keV, and the minimal angular momentum quantum number $l_{\min}$ carried out by the emitted α particle obeying the law of conservation of angular momentum [26], respectively. The uncertainty for α decay energy is calculated by the error in the mass based on the error transmission function. The fifth and sixth columns show the experimental α decay half-lives and calculated results (including the corresponding uncertainty contributed by uncertainty of α decay energy), respectively. The next column denotes the extracted α preformation probability P_α. The last column is the ratios of P_α^{low} to P_α^{high}. P_α^{low} and P_α^{high} denote the α preformation probability of nuclei where the unpaired nucleon occupies the low and high angular momentum orbit, corresponding to the low and high spin states, respectively.

From Tables 1–3, we can see the α preformation probabilities P_α are far less than 1, except for some nuclei, such as ^{167}Re, ^{149}Tb$^{\mathrm{m}}$, ^{209}Ra$^{\mathrm{m}}$ and so on. This indicates that there may be some errors in the experimental data or the complex nuclear structure of these nuclei are very different. Besides, the α decay energy and half-life of ground states are almost the same as those of the corresponding low-lying isomeric states. Especially, some isomeric states are more stable for α decay than the corresponding ground states, e.g. ^{155}Lu$^{\mathrm{m}}$, ^{191}Pb$^{\mathrm{m}}$, ^{197}Au$^{\mathrm{m}}$ and so on. The ratios of P_α^{low} to P_α^{high} are around 1, which shows the α preformation probability of isomeric state is similar to that of the ground state. This conclusion is consistent with Ref. [27]. We can also see that the calculated results of α decay half-lives can reproduce the experimental data well.

In our mind, the spin-parity state of the parent nucleus possibly plays a role in the α preformation probability due to spin dependence of the nuclear force. The α preformation probability depends on the binding energy of nucleons that eventually form the α particle [28]. The greater the α particle separation energy of the parent nucleus, the smaller the α preformation probability is. In the following, we focus on the effects of the spin-parity state of the parent nucleus on the α preformation probability.

In Table 1, all the parent nuclei are odd(Z)-even(N) nuclei below the $Z = 82$ closed shell. In this condition, $1/2^+$ and $11/2^-$ are quasi-degenerate proton levels [7]. In Table 2, all the parent nuclei are even(Z)-odd(N) nuclei below the $N = 126$ shell closure, where the quasi-degenerate neutron levels are $13/2^+$ and $1/2^-$. Interestingly, in some cases, the sequence of levels between the α decay parent and daughter nucleus has changed. For example, $11/2^-$ is the first excited state as usual for ^{159}Ta, with excitation energy of 64 keV, while for the daughter nucleus ^{155}Lu $1/2^+$ is a higher level than $11/2^-$ with excitation energy of 20 keV and longer half-life [29]. It implies the existence of the strong spin-orbit interaction below $Z = 82$. Note that most of the ratios of low to high spin state are less than 1, which indicates the α preformation probability of high spin states is larger than that of the low ones. That could be because of the difference of pairing energy at different levels. It has been shown that the pairing energy at high angular momentum orbit is bigger than that of low j orbit [30].

Table 1. Calculations of α decay half-lives and the α particle preformation probabilities of both nuclear isomers and ground states, including nuclei below the $Z=82$ shell closure.

α transition	$I_i^\pi \rightarrow I_j^\pi$	Q_α/keV	$l_{\min}$	$T_{1/2}^{\mathrm{expt}}$	$T_{1/2}^{\mathrm{calc}}$	P_α	$P_\alpha^{\mathrm{low}}/P_\alpha^{\mathrm{high}}$
$^{177}\mathrm{Au}\rightarrow^{173}\mathrm{Ir}\rightarrow^{169}\mathrm{Re}\rightarrow^{165}\mathrm{Ta}$							
$^{177}\mathrm{Au}\rightarrow^{173}\mathrm{Ir}$	$(1/2^+,3/2^+)\rightarrow(1/2^+,3/2^+)$	6298±15	0	3.65 s	$1.23^{+0.20}_{-0.16}$ s	0.12	-
$^{177}\mathrm{Au}^{\mathrm{m}}\rightarrow^{173}\mathrm{Ir}^{\mathrm{m}}$	$11/2^-\rightarrow(11/2^-)$	6261±15	0	1.79 s	$1.73^{+0.26}_{-0.23}$ s	0.34	0.35
$^{173}\mathrm{Ir}\rightarrow^{169}\mathrm{Re}^{\mathrm{m}}$	$(1/2^+,3/2^+)\rightarrow(1/2^+,3/2^+)$	5541±16	0	129 s	290^{+56}_{-46} s	0.79	-
$^{173}\mathrm{Ir}^{\mathrm{m}}\rightarrow^{169}\mathrm{Re}$	$(11/2^-)\rightarrow(9/2^-)$	5942±18	2	18.3 s	$90.1^{+1.5}_{-1.6}$ s	0.17	4.57
$^{169}\mathrm{Re}\rightarrow^{165}\mathrm{Ta}^{\mathrm{m}}$	$(9/2^-)\rightarrow(9/2^-)$	4989±18	0	45 hr	$5.09^{+1.29}_{-1.01}$ hr	0.04	-
$^{169}\mathrm{Re}^{\mathrm{m}}\rightarrow^{165}\mathrm{Ta}$	$(1/2^+,3/2^+)\rightarrow(1/2^+,3/2^+)$	5189±22	0	2.1 hr	$27.4^{+8.0}_{-6.2}$ min	0.08	1.92
$^{177}\mathrm{Tl}\rightarrow^{173}\mathrm{Au}\rightarrow^{169}\mathrm{Ir}\rightarrow^{165}\mathrm{Re}$							
$^{177}\mathrm{Tl}\rightarrow^{173}\mathrm{Au}$	$(1/2^+)\rightarrow(1/2^+)$	7066±33	0	24.7 ms	$15.7^{+4.3}_{-3.5}$ ms	0.22	-
$^{177}\mathrm{Tl}^{\mathrm{m}}\rightarrow^{173}\mathrm{Au}^{\mathrm{m}}$	$(11/2^-)\rightarrow(11/2^-)$	7654±23	0	367 us	201^{+35}_{-30} us	0.19	1.16
$^{173}\mathrm{Au}\rightarrow^{169}\mathrm{Ir}$	$(1/2^+)\rightarrow(1/2^+)$	6837±35	0	29.1 ms	$15^{+4.9}_{-3.7}$ ms	0.18	-
$^{173}\mathrm{Au}^{\mathrm{m}}\rightarrow^{169}\mathrm{Ir}^{\mathrm{m}}$	$(11/2^-)\rightarrow(11/2^-)$	6896±24	0	15.7 ms	$9.39^{+2.0}_{-1.5}$ ms	0.21	0.86
$^{169}\mathrm{Ir}\rightarrow^{165}\mathrm{Re}$	$(1/2^+)\rightarrow(1/2^+)$	6141±35	0	784 ms	882^{+342}_{-242} ms	0.39	-
$^{169}\mathrm{Ir}^{\mathrm{m}}\rightarrow^{165}\mathrm{Re}^{\mathrm{m}}$	$(11/2^-)\rightarrow(11/2^-)$	6266±24	0	390 ms	$282^{+68.1}_{-54.7}$ ms	0.25	1.56
$^{175}\mathrm{Au}\rightarrow^{171}\mathrm{Ir}\rightarrow^{167}\mathrm{Re}\rightarrow^{163}\mathrm{Ta}$							
$^{175}\mathrm{Au}\rightarrow^{171}\mathrm{Ir}$	$1/2^+\rightarrow1/2^+$	6575±57	0	216 ms	$119^{75.3}_{-45.8}$ ms	0.19	-
$^{175}\mathrm{Au}^{\mathrm{m}}\rightarrow^{171}\mathrm{Ir}^{\mathrm{m}}$	$(11/2^-)\rightarrow(11/2^-)$	6585±57	0	179 ms	$109^{+71.9}_{-41.7}$ ms	0.21	0.90
$^{171}\mathrm{Ir}\rightarrow^{167}\mathrm{Re}^{\mathrm{m}}$	$1/2^+\rightarrow1/2^+$	5855±57	0	3.1 s	$12.3^{+9.52}_{-5.32}$ s	1.39	-
$^{171}\mathrm{Ir}^{\mathrm{m}}\rightarrow^{167}\mathrm{Re}$	$(11/2^-)\rightarrow(9/2^-)$	6155±57	2	2.72 s	$1.31^{+0.92}_{-0.53}$ s	0.17	8.28
$^{167}\mathrm{Re}\rightarrow^{163}\mathrm{Ta}^{\mathrm{m}}$	$(9/2^-)\rightarrow(9/2^-)$	5145±57	0	3.4 s	$51.4^{+50.3}_{-25.1}$ min	317.61	-
$^{167}\mathrm{Re}^{\mathrm{m}}\rightarrow^{163}\mathrm{Ta}$	$1/2^+\rightarrow1/2^+$	5405±57	0	590 s	$158^{+140}_{-73.7}$ s	0.09	0
$^{167}\mathrm{Ir}\rightarrow^{163}\mathrm{Re}\rightarrow^{159}\mathrm{Ta}\rightarrow^{155}\mathrm{Lu}\rightarrow^{151}\mathrm{Tm}$							
$^{167}\mathrm{Ir}\rightarrow^{163}\mathrm{Re}$	$1/2^+\rightarrow1/2^+$	6504±27	0	68.1 ms	$39.7^{+10.3}_{-8.13}$ ms	0.20	-
$^{167}\mathrm{Ir}^{\mathrm{m}}\rightarrow^{163}\mathrm{Re}^{\mathrm{m}}$	$11/2^-\rightarrow11/2^-$	6561±27	0	28.6 ms	$24.5^{+6.24}_{-4.9}$ ms	0.30	0.68
$^{163}\mathrm{Re}\rightarrow^{159}\mathrm{Ta}$	$1/2^+\rightarrow1/2^+$	6012±28	0	1.22 s	$0.43^{+0.13}_{-0.098}$ s	0.12	-
$^{163}\mathrm{Re}^{\mathrm{m}}\rightarrow^{159}\mathrm{Ta}^{\mathrm{m}}$	$11/2^-\rightarrow11/2^-$	6068±27	0	324 ms	$256^{+72.3}_{-56}$ ms	0.28	0.45
$^{159}\mathrm{Ta}\rightarrow^{155}\mathrm{Lu}^{\mathrm{m}}$	$1/2^+\rightarrow1/2^+$	5660±28	0	3.06 s	$1.58^{+0.50}_{-0.38}$ s	0.18	-
$^{159}\mathrm{Ta}^{\mathrm{m}}\rightarrow^{155}\mathrm{Lu}$	$11/2^-\rightarrow11/2^-$	5744±28	0	1.02 s	$0.69^{+0.22}_{-0.16}$ s	0.24	0.76
$^{155}\mathrm{Lu}\rightarrow^{151}\mathrm{Tm}$	$(11/2^-)\rightarrow(11/2^-)$	5803±28	0	76.2 ms	$48.6^{+14.6}_{-10.9}$ ms	0.22	-
$^{155}\mathrm{Lu}^{\mathrm{m}}\rightarrow^{151}\mathrm{Tm}^{\mathrm{m}}$	$(1/2^+)\rightarrow(1/2^+)$	5730±28	0	182 ms	$96.3^{+30}_{-22.3}$ ms	0.19	0.83
$^{153}\mathrm{Ho}\rightarrow^{149}\mathrm{Tb}\rightarrow^{145}\mathrm{Eu}$							
$^{153}\mathrm{Ho}\rightarrow^{149}\mathrm{Tb}^{\mathrm{m}}$	$11/2^-\rightarrow11/2^-$	4016±6	0	65.7 hr	$139^{+13.4}_{-12.4}$ hr	0.74	-
$^{153}\mathrm{Ho}^{\mathrm{m}}\rightarrow^{149}\mathrm{Tb}$	$1/2^+\rightarrow1/2^+$	4121±6	0	86.1 hr	$28.5^{+2.82}_{-2.37}$ hr	0.12	0.16
$^{149}\mathrm{Tb}\rightarrow^{145}\mathrm{Eu}$	$1/2^+\rightarrow5/2^+$	4078±5	2	24.7 hr	$7.71^{+0.57}_{-0.55}$ hr	0.11	-
$^{149}\mathrm{Tb}^{\mathrm{m}}\rightarrow^{145}\mathrm{Eu}^{\mathrm{m}}$	$11/2^-\rightarrow11/2^-$	3398±5	0	315 hr	$37.1^{+3.75}_{-3.08}$ yr	362.15	0
$^{151}\mathrm{Ho}\rightarrow^{147}\mathrm{Tb}^{\mathrm{m}}$	$11/2^{(-)}\rightarrow11/2^-\#$	4644±11	0	160 s	$99.2^{+14.6}_{-12.4}$ s	0.22	-
$^{151}\mathrm{Ho}^{\mathrm{m}}\rightarrow^{147}\mathrm{Tb}$	$1/2^{(+)}\rightarrow(1/2^+)$	4736±11	0	61.3 s	$32.5^{+4.82}_{-3.98}$ s	0.19	0.86
$^{153}\mathrm{Tm}\rightarrow^{149}\mathrm{Ho}$	$(11/2^-)\rightarrow(11/2^-)$	5248±21	0	1.63 s	$1.2^{+0.30}_{-0.24}$ s	0.26	-
$^{153}\mathrm{Tm}^{\mathrm{m}}\rightarrow^{149}\mathrm{Ho}^{\mathrm{m}}$	$(1/2^+)\rightarrow(1/2^+)$	5242±21	0	2.72 s	$1.28^{+0.31}_{-0.25}$ s	0.16	0.64

In Table 3, we list the numerical results of Bi, At and Fr isotopes of both ground and isomeric states in pairs. The single nucleon level structure of these nuclei is different from the nuclei below shell closure presented by Tables 1 and 2, as shown in Fig. 1. In one case, the unpaired nucleon occupies one of the quasi-degenerate orbits to form the ground and isomeric states for nuclei below the shell gap. In the other case, the Z=82 shell gap exists between the two orbits. Bi isotopes allow, for example, to form the ground state with proton pairs occupying the low-energy orbit below the shell gap; the isomeric state can be configured with proton pairs filling the high-energy orbit above the shell gap. Thus in the case of favored α decay, the isomeric state of the parent nucleus loses a proton pair and decays to the ground state of the daughter nucleus. Correspondingly, the ground state decays to the isomeric state.

Table 2. Calculations of α decay half-lives and the α particle preformation probabilities of both nuclear isomeric and ground states, including Hg, Pb, Po, Rn, and Ra isotopes below the $N=126$ shell closure.

α transition	$I_i^\pi\rightarrow I_j^\pi$	Q_α/keV	l_{min}	$T_{1/2}^{\mathrm{expt}}$	$T_{1/2}^{\mathrm{calc}}$	P_α	$P_\alpha^{\mathrm{low}}/P_\alpha^{\mathrm{high}}$
$^{185}\mathrm{Hg}\rightarrow{}^{181}\mathrm{Pt}$	$1/2^-\rightarrow1/2^-$	5773±22	0	818 s	$443^{+117}_{-91.4}$ s	0.19	-
$^{185}\mathrm{Hg}^{\mathrm{m}}\rightarrow{}^{181}\mathrm{Pt}^{\mathrm{m}}$	$13/2^+\rightarrow7/2^-$	5760±22	3	2.0 hr	$29.4^{+7.87}_{-6.12}$ min	0.01	22.05
$^{185}\mathrm{Pb}\rightarrow{}^{181}\mathrm{Hg}$	$3/2^-\rightarrow1/2^-$	6695±22	2	18.5 s	$1.1^{+0.24}_{-0.19}$ s	0.02	-
$^{185}\mathrm{Pb}^{\mathrm{m}}\rightarrow{}^{181}\mathrm{Hg}^{\mathrm{m}}$	$13/2^+\rightarrow13/2^+$	6555±71	0	8.14 s	$2.06^{+1.88}_{-0.96}$ s	0.09	0.23
$^{187}\mathrm{Pb}\rightarrow{}^{183}\mathrm{Hg}$	$3/2^-\rightarrow1/2^-$	6393±9	2	160 s	$15^{+1.29}_{-1.18}$ s	0.03	-
$^{187}\mathrm{Pb}^{\mathrm{m}}\rightarrow{}^{183}\mathrm{Hg}^{\mathrm{m}}$	$13/2^+\rightarrow13/2^+$	6208±17	0	153 s	$47.4^{+8.56}_{-7.18}$ s	0.11	0.3
$^{189}\mathrm{Pb}\rightarrow{}^{185}\mathrm{Hg}$	$3/2^-\rightarrow1/2^-$	5871±34	2	3.51 hr	$0.68^{+0.03}_{-0.02}$ hr	0.07	-
$^{189}\mathrm{Pb}^{\mathrm{m}}\rightarrow{}^{185}\mathrm{Hg}^{\mathrm{m}}$	$13/2^+\rightarrow13/2^+$	5807±52	0	1.08 hr	$0.726^{+0.56}_{-0.32}$ hr	0.23	0.29
$^{191}\mathrm{Pb}\rightarrow{}^{187}\mathrm{Hg}$	$3/2^-\rightarrow3/2^-$	5453±42	0	4.35 hr	$36.4^{+24.4}_{-14.3}$ hr	2.93	-
$^{191}\mathrm{Pb}^{\mathrm{m}}\rightarrow{}^{187}\mathrm{Hg}^{\mathrm{m}}$	$13/2^+\rightarrow13/2^+$	5404±34	0	182 hr	$65.6^{+33.6}_{-22.0}$ hr	0.13	23.18
$^{195}\mathrm{Po}\rightarrow{}^{191}\mathrm{Pb}$	$3/2^-\rightarrow3/2^-$	6755±57	0	4.94 s	$1.74^{+1.12}_{-0.68}$ s	0.12	-
$^{195}\mathrm{Po}^{\mathrm{m}}\rightarrow{}^{191}\mathrm{Pb}^{\mathrm{m}}$	$13/2^+\rightarrow13/2^+$	6840±40	0	2.13 s	833^{+341}_{-243} ms	0.14	0.9
$^{197}\mathrm{Po}\rightarrow{}^{193}\mathrm{Pb}$	$(3/2^-)\rightarrow(3/2^-)$	6405±103	0	122 s	$38.4^{+65.4}_{-23.8}$ s	0.11	-
$^{197}\mathrm{Po}^{\mathrm{m}}\rightarrow{}^{193}\mathrm{Pb}^{\mathrm{m}}$	$(13/2^+)\rightarrow13/2^+$	6505±127	0	30.7 s	$15.1^{+34.6}_{-10.4}$ s	0.17	0.64
$^{199}\mathrm{Po}\rightarrow{}^{195}\mathrm{Pb}$	$3/2^-\#\rightarrow3/2^-\#$	6074±33	0	1.22 hr	925^{+379}_{-267} s	0.07	-
$^{199}\mathrm{Po}^{\mathrm{m}}\rightarrow{}^{195}\mathrm{Pb}^{\mathrm{m}}$	$13/2^{(+)}\rightarrow13/2^{(+)}$	6181±33	0	1040 s	$310^{+122}_{-87.7}$ s	0.10	0.71
$^{201}\mathrm{Po}\rightarrow{}^{197}\mathrm{Pb}$	$3/2^-\rightarrow3/2^-$	5799±8	0	23 hr	$4.43^{+0.413}_{-0.382}$ hr	0.07	-
$^{201}\mathrm{Po}^{\mathrm{m}}\rightarrow{}^{197}\mathrm{Pb}^{\mathrm{m}}$	$13/2^+\rightarrow13/2^+$	5903±8	0	6.22 hr	$1.41^{+0.13}_{-0.115}$ hr	0.08	0.85
$^{203}\mathrm{Po}\rightarrow{}^{199}\mathrm{Pb}$	$5/2^-\rightarrow3/2^-$	5496±13	2	556 hr	$246^{+40.6}_{-37.2}$ hr	0.16	-
$^{203}\mathrm{Po}^{\mathrm{m}}\rightarrow{}^{199}\mathrm{Pb}^{\mathrm{m}}$	$13/2^+\rightarrow(13/2^+)$	5709±13	0	31.3 hr	$11^{+1.76}_{-1.5}$ hr	0.12	1.26
$^{195}\mathrm{Rn}\rightarrow{}^{191}\mathrm{Po}$	$(3/2^-)\rightarrow(3/2^-)$	7694±50	0	7 ms	$7.18^{+3.14}_{-2.22}$ ms	0.36	-
$^{195}\mathrm{Rn}^{\mathrm{m}}\rightarrow{}^{191}\mathrm{Po}^{\mathrm{m}}$	$(13/2^+)\rightarrow(13/2^+)$	7714±21	0	6 ms	$6.16^{+1.07}_{-0.863}$ ms	0.36	1
$^{197}\mathrm{Rn}\rightarrow{}^{193}\mathrm{Po}$	$(3/2^-)\rightarrow(3/2^-)$	7415±50	0	54 ms	$52.8^{+25.1}_{-16.9}$ ms	0.34	-
$^{197}\mathrm{Rn}^{\mathrm{m}}\rightarrow{}^{193}\mathrm{Po}^{\mathrm{m}}$	$(13/2^+)\rightarrow(13/2^+)$	7505±71	0	25.6 ms	$26.3^{+19.2}_{-10.9}$ ms	0.36	0.95
$^{203}\mathrm{Rn}\rightarrow{}^{199}\mathrm{Po}$	$3/2^-\#\rightarrow3/2^-\#$	6630±33	0	66.7 s	$29.9^{+10.7}_{-7.89}$ s	0.16	-
$^{203}\mathrm{Rn}^{\mathrm{m}}\rightarrow{}^{199}\mathrm{Po}^{\mathrm{m}}$	$13/2^{(+)}\rightarrow13/2^{(+)}$	6680±33	0	35.9 s	$18.9^{+6.66}_{-4.94}$ s	0.18	0.85
$^{203}\mathrm{Ra}\rightarrow{}^{199}\mathrm{Rn}$	$(3/2^-)\rightarrow(3/2^-)$	7745±100	0	36 ms	$22.3^{+24.9}_{-11.6}$ ms	0.22	-
$^{203}\mathrm{Ra}^{\mathrm{m}}\rightarrow{}^{199}\mathrm{Rn}^{\mathrm{m}}$	$(13/2^+)\rightarrow(13/2^+)$	7765±42	0	25 ms	$19.2^{+7}_{-5.1}$ ms	0.27	0.81
$^{209}\mathrm{Ra}\rightarrow{}^{205}\mathrm{Rn}$	$5/2^-\rightarrow5/2^-$	7135±71	0	5.23 s	$2.07^{+1.7}_{-0.938}$ s	0.14	-
$^{209}\mathrm{Ra}^{\mathrm{m}}\rightarrow{}^{205}\mathrm{Rn}^{\mathrm{m}}$	$13/2^+\rightarrow13/2^+\#$	7355±71	0	0.13 ms	341^{+254}_{-152} ms	918.62	0

The results for high and low spin states in Table 3 seem to contradict the previous conclusion that nuclei in high-spin states have large preformation probabilities. Unlike the quasi-degenerate levels in a single shell, in this case the orbits are separated by a shell gap. Clearly, nucleon pairs in the outer space are active and weakly bound to the inert nuclear core. Thus the α preformation probabilities of nuclear isomers with nucleon pairs filling the outer orbit are larger than that of the corresponding ground states, as shown in Fig. 1. The $9/2^-$ orbit is a higher level than the $1/2^+$ orbit, thus the α preformation probability of the $1/2^+$ configuration is larger than that of the $9/2^-$ configuration.

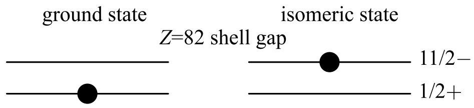

(a) below Z=82 closed shell

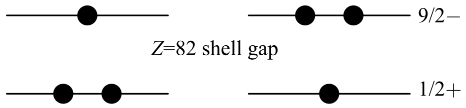

(b) cross Z=82 closed shell

Fig. 1. Schematic diagram of single nucleon level structure for nuclei around the Z=82 closed shell, including (a) the levels below shell gap, (b) the levels cross shell gap.

Table 3. Calculations of α decay half-lives and the α particle preformation probabilities of both nuclear isomeric and ground states, including Bi, At, and Fr isotopes above the $Z=82$ shell closure.

α transition	$I_i^\pi \to I_j^\pi$	Q_α/keV	$l_{\min}$	$T_{1/2}^{\mathrm{expt}}$	$T_{1/2}^{\mathrm{calc}}$	P_α	$P_\alpha^{\mathrm{low}}/P_\alpha^{\mathrm{high}}$
^{187}Bi→^{183}Tl$^{\mathrm{m}}$	$(1/2^-,5/2^-)\to3/2^-$	7151±13	2	37 ms	$63.4^{+6.88}_{-6.20}$ ms	0.60	-
^{187}Bi$^{\mathrm{m}}$→^{183}Tl	$13/2^+\#\to13/2^+$	7887±15	0	370 us	$159^{+17}_{-15.4}$ us	0.15	3.99
^{189}Bi→^{185}Tl$^{\mathrm{m}}$	$(9/2^-)\to9/2^-\#$	6813±30	0	658 ms	505^{+152}_{-114} ms	0.27	-
^{189}Bi$^{\mathrm{m}}$→^{185}Tl	$(1/2^+)\to1/2^+\#$	7452±30	0	9.8 ms	$3.12^{+0.771}_{-0.625}$ ms	0.11	0.41
^{191}Bi→^{187}Tl$^{\mathrm{m}}$	$(9/2^-)\to(9/2^-)$	6443±11	0	24.3 s	$12.3^{+1.3}_{-1.23}$ s	0.18	-
^{191}Bi$^{\mathrm{m}}$→^{187}Tl	$(1/2^+)\to(1/2^+)$	7018±12	0	182 ms	$81.7^{+8.96}_{-7.55}$ ms	0.16	0.88
^{193}Bi→^{189}Tl$^{\mathrm{m}}$	$(9/2^-)\to9/2^{(-)}$	6021±14	0	30.3 min	$700^{+111}_{-94.3}$ s	0.13	-
^{193}Bi$^{\mathrm{m}}$→^{189}Tl	$(1/2^+)\to(1/2^+)$	6613±16	0	3.81 s	$2.34^{+0.361}_{-0.312}$ s	0.21	1.59
^{195}Bi→^{191}Tl^{m}	$(9/2^-)\to9/2^{(-)}$	5535±9	0	169 hr	$37.8^{+4.38}_{-3.83}$ hr	0.08	-
^{195}Bi$^{\mathrm{m}}$→^{191}Tl	$(1/2^+)\to(1/2^+)$	6232±11	0	264 s	$74.9^{+8.48}_{-7.83}$ s	0.10	1.28
^{197}Bi→^{193}Tl$^{\mathrm{m}}$	$(9/2^-)\to(9/2^-)$	4993±11	0	17.8 yr	$3.96^{+0.65}_{-0.563}$ yr	0.08	-
^{197}Bi$^{\mathrm{m}}$→^{193}Tl	$(1/2^+)\to1/2^{(+\#)}$	5897±11	0	550 s	2080^{+259}_{-230} s	1.33	16.98
^{191}At→^{187}Bi$^{\mathrm{m}}$	$(1/2^+)\to1/2^+\#$	7714±20	0	2.1 ms	$2.9^{+0.452}_{-0.385}$ ms	0.48	-
^{191}At$^{\mathrm{m}}$→^{187}Bi	$(7/2^-)\to9/2^-\#$	7880±21	2	2.2 ms	$1.6^{+0.251}_{-0.22}$ ms	0.25	1.9
^{193}At→^{189}Bi$^{\mathrm{m}}$	$1/2^+\#\to(1/2^+)$	7388±30	0	29 ms	$29.7^{+7.88}_{-6.07}$ ms	0.36	-
^{193}At$^{\mathrm{m}}$→^{189}Bi	$7/2^-\#\to(9/2^-)$	7581±30	2	21 ms	$12.4^{3.08}_{-2.49}$ ms	0.21	1.74
^{197}At→^{193}Bi	$(9/2^-)\to(9/2^-)$	7108±51	0	404 ms	$222^{+117}_{-75.5}$ ms	0.19	-
^{197}At$^{\mathrm{m}}$→^{193}Bi$^{\mathrm{m}}$	$(1/2^+)\to(1/2^+)$	6846±18	0	2 s	$2.03^{+0.351}_{-0.278}$ s	0.36	1.85
^{201}Fr→^{197}At	$(9/2^-)\to(9/2^-)$	7515±86	0	62 ms	$53.1^{+50.5}_{-25.6}$ ms	0.30	-
^{201}Fr$^{\mathrm{m}}$→^{197}At$^{\mathrm{m}}$	$(1/2^+)\to(1/2^+)$	7608±52	0	27 ms	$26.1^{+12.6}_{-8.3}$ ms	0.34	1.13

4 Summary

In summary, we have performed calculations on α decay half-lives and preformation probabilities within the two-potential approach. The results, that the α preformation probabilities of nuclear isomers are similar to those of ground states, are in line with previous work. For nuclei below the $Z = 82$ and $N = 126$ closed shells alike, the existence of quasi-degenerate levels results in low lying isomeric and ground states. The α preformation probability of nuclei in high-spin states seem to be larger than that in low-spin states. Moreover, nuclei with nucleon number slightly above the magic numbers, such as Bi, At and Fr isotopes, have a special model of excitation. In their isomeric states, proton pairs outside the inert nuclear core are active and can easily preform the α particle.

References

1 P. M. Walker and J. J. Carroll, Phys. Today, **58**: 39–44 (2005)
2 F. R. Xu, E. G. Zhao, R. Wyss et al, Phys. Rev. Lett., **92**: 107–110 (2004)
3 A. Aprahamian and Y. Sun, Nature Phys., **1**: 81–82 (2005)
4 M. Block, C. Bachelet, G. Bollen et al, Phys. Rev. Lett., **100**: 3182–3186 (2008)
5 E. Peik and Z. Kai, Phys. Rev. Lett., **109**: 3076–3080 (2012)
6 R. D. Herzberg, P. T. Greenlees, P. A. Butler et al, Nature, **442**: 896 (2006)
7 G. Audi, F. G. Kondev, M. Wang et al, Chin. Phys. C, **36**: 1157–1286 (2012)
8 A. N. Andreyev, M. Huyse, P. V. Duppen et al, Nature, **405**: 430–433 (2000)
9 D. S. Delion, S. Peltonen and J. Suhonen, Phys. Rev. C, **73**: 4315 (2006)
10 W. M. Seif, Phys. Rev. C, **74**: 140–143 (2006)
11 D. Ni and Z. Ren, Chin. Phys. Lett., **30**: 22101–22104 (2013)
12 Y. Ren and Z. Ren, Phys. Rev. C, **85**: 044608 (2012)
13 H. F. Zhang, G. Royer, and J. Q. Li, Phys. Rev. C, **84**: 027303 (2011)
14 Y. Qian and Z. Ren, Sci. Chin. Phys. Mech. Sastro., **56**: 1520–1524 (2013)
15 W. M. Seif, Phys. Rev. C, **91**: 014322 (2015)
16 C. Xu, Z. Ren, G. Röpke et al, Phys. Rev. C, **93**: 011306(R) (2016)
17 C. Qi, Rev. Phys., **1**: 77–89 (2016)
18 S. A. Gurvitz and G. Kalbermann, Phys. Rev. Lett., **59**: 262–265 (1987)
19 X. J. Bao, S. Q. Guo, H. F. Zhang et al, J. Phys. G: Nucl. Part. Phys., **42**: 085101 (2015)
20 M. Gonçalves and S. B. Duarte, Phys. Rev. C, **48**: 2409–2414 (1993)
21 G. Gamow, Z. Phys. A, **52**: 726–734 (1928)
22 B. Buck, A. C. Merchant, and S. M. Perez, Phys. Rev. C, **45**:2247–2253 (1992)
23 G. Royer, J. Phys. G: Nucl. Part. Phys., **26**: 1149–1170 (2000)
24 X. D. Sun, P. Guo and X. H. Li, Phys. Rev. C, **93**: 034316 (2016)
25 C. Xu and Z. Ren, Nucl. Phys. A, **760**: 303–316 (2005)
26 V. Yu. Denisov, and A. A. Khudenko, Phys. Rev. C, **79**: 054614 (2009)
27 J. Dong, H. Zhang, Y. Wang et al, Nucl. Phys. A, **832**: 198–208 (2010)
28 D. Deng and Z. Ren, Phys. Rev. C, **93**: 044326 (2016)
29 www.nndc.bnl.gov
30 J. Hu, B. Yang, and C. Zheng and *Nuclear Physics Theory* (Beijing: Atomic Energy Press, 1993), p. 53